

A new photonic crystal fiber gas sensor based on evanescent wave in terahertz wave band: design and simulation*

ZHANG Li (张丽)¹, REN Guang-jun (任广军)^{1**}, and YAO Jian-quan (姚建铨)²

1. Tianjin Key Lab. of Film Electronic & Communication Devices, Engineering Research Center of Communication Devices and Technology, Ministry of Education of China, Institute of Electronics Information Engineering, Tianjin University of Technology, Tianjin 300384, China

2. Key Laboratory of Optoelectronics Information and Technical Science, Ministry of Education of China, Institute of Laser and Optoelectronics, College of Precision Instrument and Optoelectronics Engineering, Tianjin University, Tianjin 300072, China

(Received 3 September 2013; Revised 8 September 2013)

©Tianjin University of Technology and Springer-Verlag Berlin Heidelberg 2013

In this paper, we present the design of a new photonic crystal fiber (PCF) gas sensor for evanescent-field sensing in terahertz (THz) wave band. This sensor can be used to identify the gas, and its size is very large, so that it is beneficial to fill it with the test substance. Based on simulation, we demonstrate that the gas sensor using PCFs with four noncircular large holes in the cladding has high sensitivity and low loss, the confinement loss is less than 0.007 dB/m, and the bending loss is very small. The new PCF gas sensor can detect kinds of gases, for example, if test gas is water vapor, it has obvious absorption peaks in THz band, and the sensitivities of gas sensor are 64% and 73% at 1.097 THz and 0.752 THz, respectively. Due to the ultra-low loss and high sensitivity of the model, the novel steering-wheel structured fiber is very suitable for evanescent-field sensing and the detection of chemical and biological products.

document code: A **Article ID:** 1673-1905(2013)06-0438-3

DOI 10.1007/s11801-013-3157-5

Due to the unique structure features and novel optical characteristics, photonic crystal fiber (PCF) has been increasingly explored for a large variety of applications ranging from communications to sensing^[1-6]. PCF sensing platform based on evanescent field is of particular interest for chemical and biological sensing and detection^[7,8]. In 2006, a novel gas sensor with total internal reflection-type PCF has been proposed by Cordeiro et al^[9]. PCF has a wide application in the field of terahertz (THz) evanescent-field sensing^[10], and it provides a very flexible route towards THz wave guiding. Nowadays, many researches on the use of the evanescent field for gas detection have been reported^[11,12], and the PCF shows a great potential in sensing applications. However, besides the popularity of evanescent-field sensing modality for fiber optic sensors, it continues to face the challenge of insufficient mode-field overlap with measurands, thus the sensitivity is limited, and the highest relative sensitivity of traditional PCF reported currently is still very low^[13]. An effective way to increase the sensitivity is to design new PCF structures. In this paper, a new PCF gas sensor based on evanescent-field sensing is designed.

Optimal light intensity overlap in air hole is theoretically realized. Compared with traditional sensor, the new PCF gas sensor has higher sensitivity and lower loss. The background material is polymethyl-methacrylate (PMMA) in optical fiber, because THz transmission losses in plastic are very small, and plastic which can be used in harsh environment is flexible compared with silicon. We predict theoretically that the optimal evanescent-field sensing structure can be achieved by adjusting the corresponding parameters, such as web thickness, core diameter and air hole size.

The design is based on an effective step-index model derived from classical fiber optics theory, so that the traditional numerical approaches can be used for the description of the new PCF gas sensor. Such a design can achieve an air-filling fraction of about 93%. The configuration of the new PCF gas sensor is shown in Fig.1. There are four noncircular large air holes in the cladding layer. The diameter of minimum air holes r_1 is 30 μm , the hole pitch A is 35 μm , r_2 is 0.12 mm, R_1 is 0.866 mm, R_2 is 0.894 mm, R_3 is 0.954 mm, and web thickness d is ranging from 21 μm to 23 μm located in the model center parts.

* This work has been supported by the National Basic Research Program of China (No.2010CB327801).

** E-mail: rgj1@163.com

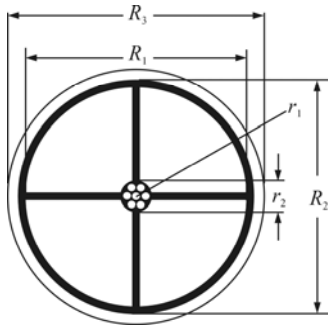


Fig.1 The configuration of the low-loss PCF gas sensor

The near-field image of the new PCF gas sensor is shown in Fig.2. It is modeled using beam propagation method that allows analyses of the fundamental mode in core and its optical properties. The sensitivity of the model depends on the power ratio of input light and evanescent wave. The new PCF gas sensor allows a guided mode to overlap with adjacent air holes more efficiently, because sufficient surface area of core is exposed to the evanescent field in this paper. Therefore, the sensitivity of this model is greater than that of traditional PCF. The new PCF gas sensor is a total internal reflection-type PCF which is characterized by guided-mode optical power concentrated at the center of the defects, while only a very small part of the optical energy (evanescent wave) distributes in the noncircular large air holes.

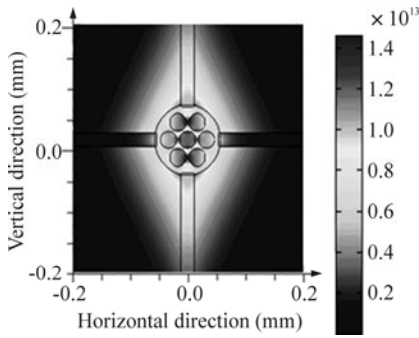


Fig.2 Near-field image of the new PCF gas sensor with noncircular air holes in the cladding ($\lambda=0.3$ mm)

Sensitivity is an important parameter in the sensor based on evanescent wave. Here we calculate the field distribution and analyze the evanescent field in PCF. The numerical calculation formula of sensitivity is given by

$$r_f = f n_r / n_e, \tag{1}$$

where n_r is the refractive index of the filling substance, n_e is the guide-mode effective refractive index, and r_f is the relative sensitivity coefficient. For the new PCF gas sensor model, f is the ratio of the optical power within the noncircular large air holes to the total power, using the Poynting's theorem, which can be expressed as

$$f = \int_{\text{holes}} (E_x H_y - E_y H_x) dx dy / \int_{\text{total}} (E_x H_y - E_y H_x) dx dy, \tag{2}$$

where E_x, E_y, H_x and H_y express transverse and longitudinal electric and magnetic field model components, respectively. In this paper, the data are obtained by COMSOL Multiphysics 3.5.

We obtain the power percentage in noncircular large holes versus frequency with web thicknesses d ranging from 21 μm to 23 μm , as shown in Fig.3. The power percentage decreases with the increase of frequency. And at the same frequency, the power percentage decreases with the increase of web thickness d . In the case of web thickness d as 23 μm , the power percentage in noncircular large air holes is 72% when the incident frequency is 1 THz. We can detect many kinds of gases. For example, water vapor has obvious absorption peaks in THz band, so if the test gas is water vapor, the evanescent wave will be absorbed by water vapor, and the sensitivities of the gas sensor for water vapor are 64% and 73% at 1.097 THz and 0.752 THz, respectively. We can select appropriate structural parameters and working frequency for the new PCF gas sensor according to the requirement of power percentage in practice.

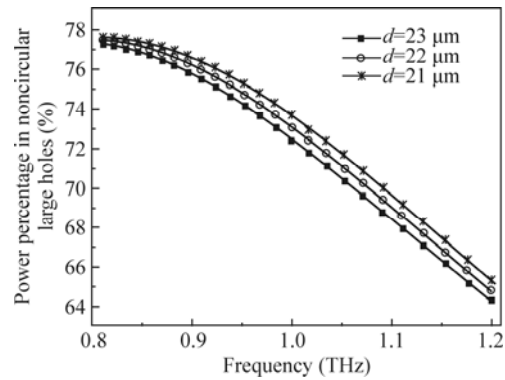


Fig.3 The power percentage in noncircular large air holes vs. frequency for different web thicknesses of 23 μm , 22 μm and 21 μm

The traditional fiber loss in the past few decades has been constantly reduced, and it is increasingly difficult to further reduce the traditional optical fiber loss. In this paper, we analyze the confinement loss in the PCF by finite element method. The confinement loss is defined as

$$CL(\text{dB/m}) = 40\pi \times \text{Im}(n_{\text{eff}}) / (\lambda \ln 10), \tag{3}$$

where λ is the input wavelength, and $\text{Im}(n_{\text{eff}})$ is the imaginary part of the effective refractive index of the fundamental mode. According to Eq.(3), the confinement loss depends on two variables, namely wavelength and the imaginary part of effective refractive index, respectively. However, the imaginary part of effective refractive index is a function of wavelength too.

The confinement loss is calculated for different d values of 21 μm , 22 μm and 23 μm , and the results are shown in Fig.4. The minimum confinement loss is as low as 0.007 dB/m. For a particular d , there is a critical frequency, before which the confinement loss decreases sharply with the increase of frequency. This critical frequency decreases with the increase of d .

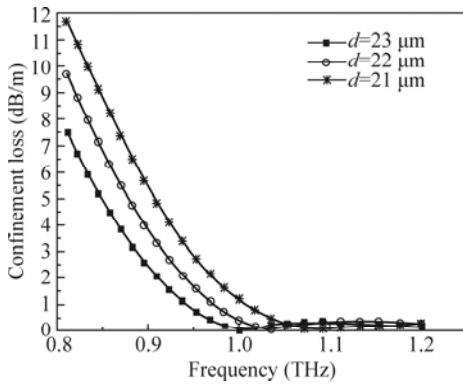


Fig.4 Confinement loss vs. frequency for different web thicknesses of 23 μm, 22 μm and 21 μm

Predictions of macro-bending induced attenuation in PCFs have been made by using various approaches. Here, the bending loss is defined as^[14]

$$\alpha A \approx A^2 \times \lambda / (8\sqrt{6\pi} \times n_s \times A_{\text{eff}}) \times F[R / (6\pi^2 \times n_s^2 \times A)(\lambda / A)^2 V_{\text{PCF}}^3], \quad (4)$$

$$F(x) = x^{-1/2} \exp(-x), \quad (5)$$

where α is bending loss, n_s is the index of PMMA, R is the bending radius, A_{eff} is the effective area, and $V_{\text{PCF}} = 2\pi A / \lambda \times [n_{\text{co}}^2(\lambda) - n_{\text{cl}}^2(\lambda)]^{1/2}$, n_{co} is the core index, and n_{cl} is the cladding index. The results are shown in Fig.5. For a particular R , there is a critical frequency, above which the micro-bending loss begins to increase sharply. This critical frequency increases with the increase of R . The micro-bending loss of the new PCF gas sensor is negligible.

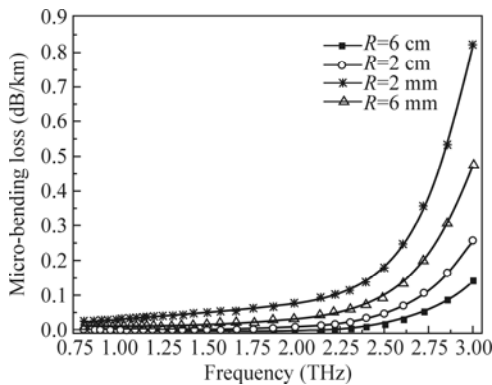


Fig.5 Micro-bending loss vs. frequency for different bending radii

We present a PCF gas sensor model. The confinement loss is as low as 0.007 dB/m, and the power percentage in noncircular large air holes is 72% when the incident frequency is 1 THz. We predict theoretically that the optimal evanescent-field sensing structure can be achieved by adjusting the corresponding parameters, such as web thickness, core diameter and air hole size. The evanescent wave sensor for THz band has a certain guiding significance for the research and application.

References

- [1] H. Du, SERS-based Photonic Crystal Fiber Sensing Platform, Proc. SPIE **6083**, 74 (2006).
- [2] P. St. J. Russell, Science **299**, 358 (2003).
- [3] M. Nielsen, C. Jacobsen, N. Mortensen, J. Folkenberg and H. Simonsen, Optics Express **12**, 1372 (2004).
- [4] B. Temelkuran, S. D. Hart, G. Benoit, J. D. Joannopoulos and Y. Fink, Nature **420**, 650 (2002).
- [5] BING Pi-bin, LI Jian-quan, LU Ying, DI Zhi-gang and YAN Xin, Optoelectronics Letters **8**, 0245 (2012).
- [6] Yuan Yin-Quan, Guo Zhen-Qiang and Ding Li-Yun, Optoelectronics Letters **6**, 346 (2010).
- [7] M. N. Petrovich, A. van Brakel, F. Poletti, K. Mukasa, E. Austin, V. Finazzi, P. Petropoulos, E. O. Driscoll, M. Watson, T. DelMonte, T. M. Monro, J. P. Dakin and D. J. Richardson, Microstructured Fibers for Sensing Applications, Proc. SPIE **6005**, 60050E (2005).
- [8] T. Ritari, J. Tuominen, H. Ludvigsen, J. C. Petersen, T. Sorensen, T. P. Hansen and H. R. Simonsen, Optics Express **12**, 4080 (2004).
- [9] C. M. B. Cordeiro, M. A. R. Franco, G. Chesinil, E. S. C. Barretto, R. Lwin, C. H. B. Curz and M. C. J. Large, Optics Express **14**, 13056 (2006).
- [10] B. Ung, A. Dupuis, K. Stoeffler, C. Dubois and M. Skorobogatiy, Opt. Soc. Am. B **28**, 917 (2011).
- [11] T. M. Monro, D. J. Richardson and P. J. Bennett, Electron. Lett. **35**, 1188 (1999).
- [12] Y. L. Hoo, W. Jin, H. L. Ho, D. N. Wang and R. S. Windeler, Opt. Eng. **41**, 8 (2002).
- [13] Y. L. Hoo, W. Jin, C. Shi, H. L. Ho, D. N. Wang and S.C. Ruan, Appl. Opt. **42**, 3509 (2003).
- [14] M. D. Nielsen, N. A. Mortensen, M. Albertsen, J. R. Folkenberg, A. Bjarkley and D. Bonacinni, Opt. Express **12**, 1775 (2004).